Ag Nanoparticle Green Synthesis using *Litchi chinensis* Peels Extract: Mutagenicity, Cytotoxicity, Antimicrobial and Antioxidant Activities Evaluation

[1]Mazhar Abbas**, [1,2]Aqsa Mumtaz, [3]Norah Alwadai, [4,5,6]Munawar Iqbal*, [7]Arif Nazir, [8]Ismat Bibi, [7]Abid Ali, [6]Naveed Ahmad and [3]Maryam Al Huwayz

[1]*Section of Biochemistry, Department of Basic Sciences, College of Veterinary and Animal Sciences (CVAS) Jhang, University of Veterinary and Animal Sciences (UVAS), Lahore, Pakistan.*

[2]*School of Chemistry, Xian Jiatong University Xi'an, Shaanxi, 710049, China.*

[3]*Department of Physics, College of Sciences, Princess Nourah bint Abdulrahman University, P.O. Box 84428, Riyadh 11671, Saudi Arabia.*

[4]*Renewable Energy and Environmental Technology Center, University of Tabuk, Tabuk, 47913, Saudi Arabia.*

[5]*School of Chemistry, University of the Punjab, Lahore 54590, Pakistan.*

[6]*Department of Chemistry, Division of Science and Technology, University of Education, Lahore, Pakistan.*

[7]*Department of Chemistry, The University of Lahore, Lahore, Pakistan.*

[8]*Institute of Chemistry, The Islamia University of Bahawalpur, Bahawalpur, Pakistan.*

bosalvee@yahoo.com*; mazhar.abbas@uvas.edu.pk**

(Received on 9th May 2025, accepted in revised form 1st December 2025)

Summary: In view of the promising therapeutic potential of AgNPs, in the present study, the cytotoxicity of AgNPs was evaluated against HepG2, which were prepared using *Litchi chinensis* peels (LCP) extract. The mutagenicity, antimicrobial and antioxidant activities were also evaluated. The AgNPs showed favorable antioxidant activity, i.e., total phenolic contents (TPC) (48.46 mg GAE/g DW), total flavonoid contents (TFC) (35.83 mg CE/g DW) and free radical scavenging (84.93% inhibition). The antibacterial activity was assessed against *E. coli, B. subtilis, P. multocida,* and *S. aureus* bacterial strains, which also revealed promising antibacterial activity. The FTIR analysis revealed the involvement of phytochemicals in the formation of AgNPs. The SEM analysis revealed the formation of semi-spherical particles with a tendency to aggregate, which was due to the interactions among biomolecules on the surface of particle. The AgNPs was in a face-centered cubic (FCC) crystal structure. The AgNPs showed no apparent toxicity against HepG2 cells. Additionally, mutagenicity was evaluated against *S. typhi* of TA98 and TA100 strains, which revealed the non-mutagenic nature of the AgNPs. The LCP-AgNPs demonstrated promising potential for biomedical applications.

Keywords: Green synthesis, *Litchi chinensis* peel, AgNPs, antibacterial activity, antioxidant activity, cytotoxicity, mutagenicity.

Introduction

In the current scientific and technological era, nanotechnology is becoming more and more common. Because of their many beneficial qualities, such as targeted drug delivery, therapeutic potential, diagnostic capabilities, and regenerative medicine applications, nanoparticles are becoming more and more popular in biomedical research. Nanoparticles are divided into four different nanosystems based on their physicochemical characteristics: alloy nanoparticles, metallic nanoparticles, metal oxide nanoparticles, and magnetic nanoparticles [1-3]. Because of their non-toxicity, bioactivity, and biocompatibility, metal nanoparticles are utilized in the biological field [4]. Additionally, by encapsulating therapeutic agents in particular cells and organelles, nanoparticles improve the targeted delivery of medications, helping to treat a variety of illnesses [5].

In living systems, oxidation is crucial because it supplies the energy required for a variety of biological processes. An imbalance arises, though, when the body's ability to neutralize reactive species is outpaced by their generation. Oxidative stress is a condition that can damage essential cellular components, such as proteins, lipids, and genetic material. This imbalance leads to genotoxic stress, which includes abnormal gene expression, alterations in DNA sequence, chromosomal structure, and cell phenotypes [6]. By controlling gene expression and stabilizing reactive oxygen species (ROS), phenolic compounds derived from plants have a great potential

*To whom all correspondence should be addressed.

to lessen oxidative damage. Important secondary metabolites in plants, phenols and flavonoids, have strong anti-genotoxic qualities. Their capacity to combat oxidative stress and affect the activity of enzymes involved in the activation of genotoxic compounds and the detoxification of their reactive intermediates accounts for their protective effects [7-10]. Researchers are increasingly looking into using these compounds in the environmentally friendly synthesis of nanoparticles because of their antioxidant potential.

Because of their cost-effectiveness and environmental friendliness, recent developments in nanotechnology have focused on the green synthesis of nanoparticles [11-15]. By using natural, non-toxic, and renewable resources like microorganisms, plant extracts, and biomolecules, biosynthetic processes lessen their impact on the environment and their dependency on dangerous chemicals. These methods contribute to the overall sustainability of nanomaterial production since they frequently use environmentally friendly processes and bio-based materials. Furthermore, because they use readily available and reasonably priced natural sources rather than pricey equipment and chemicals, these techniques are frequently more affordable [7, 12].

Nanoparticles derived from plants typically exhibit high levels of biocompatibility, making them attractive options for biomedical applications like tissue regeneration, targeted drug delivery, and diagnostic imaging. Their production can also be effectively scaled up, offering a practical and eco-friendly way to produce nanoparticles on a large scale without upsetting the natural equilibrium. In addition, these techniques are flexible and adjustable to different nanoparticle sizes, shapes, and compositions, enabling the synthesis of a wide range of nanomaterials with specialized applications. Green-synthesized nanoparticles are safer for use in biomedical and environmental applications because they can significantly lower toxicity when compared to their conventionally synthesized counterparts [16, 17]. As a result, it is a viable and sustainable method for producing nanomaterials, offering notable advantages in terms of cost-effectiveness, versatility, biocompatibility, and environmental impact [18, 19].

The remarkable biocompatibility and multifunctional qualities of silver nanoparticles (AgNPs) have drawn a lot of attention. Biomedicine, wound healing, tissue engineering, and bioimaging all make extensive use of green-synthesised AgNPs. These nanoparticles can fight a variety of bacterial, fungal, and viral infections because of their potent antimicrobial activity. Because they cause cancer cells to undergo programmed cell death while posing little harm to healthy tissues, silver-based nanostructures in particular have shown promise in oncology. Additionally, they are being investigated for use in photothermal cancer treatment methods and targeted drug delivery [8, 13]. The tropical, evergreen tree *Litchi chinensis* (Litchi) belongs to the *Sapindaceae* family and is a great source of vitamins, minerals, polyphenols, and polysaccharides. Litchi fruits are used in a variety of products, such as soups, drinks, jellies and medicinal beverages [20].

However, because of its easy deterioration, the pericarp is frequently thrown away as waste, which raises environmental concerns [21]. The hunt for genoprotective agents made from plants has been sparked by the urgent need to address ecological issues as well as the growing incidence of genetic diseases. Notably, flavones in litchi fruit's pericarp have shown significant promise in the fight against human breast cancer over time [22]. The application of peel extract from *Litchi chinensis* for the production of nanoparticles has not yet been investigated, despite a great deal of research on plant-mediated AgNP synthesis.

A survey of the synthesis of AgNPs using various green agents is depicted in Table-1 and the litchi has not been used for the preparation of NPs [23] and biosynthesized AgNPs using LCP extract showed no toxicity on normal RBCs. Accordingly, LCP extracts were employed to biosynthesize AgNPs. Their biochemical properties were evaluated through total phenolic content (TPC), total flavonoid content (TFC), and DPPH radical-scavenging assays. The antimicrobial performance of the green-produced nanoparticles was further tested against selected bacterial strains, including gram-positive species (*B. subtilis* and *S. aureus*) and gram-negative species (*E. coli* and *P. multocida*). Moreover, LCP-AgNPs were screened against two mutant strains of *Salmonella typhimurium* (TA98 and TA100) to evaluate their mutagenicity. This is the first approach for the cytotoxic evaluation of biosynthesized AgNPs against HepG2 cells using the MTT assay.

Table-1: Synthesis of AgNPs using various green agents.

S. No	Synthesis agent	characterization	Properties and applications	References
1	*A. cepa* extract	SEM, EDX, and XRD	Exhibited a face-centered, nearly spherical morphology with an average diameter of about 84.8 nm, and showed notable antibacterial activity against *E. coli* and *S. aureus*.	[8]
2	*S. mollis* leaf extract	FTIR, SEM and XRD, EDX.	Displayed an average size of roughly 70 nm, showed strong antibacterial effects against B. subtilis, *E. coli, S. aureus,* and *P. multocida* and demonstrated notable antioxidant capacity (TPC, TFC, DPPH) along with efficient degradation of methylene blue (MB) dye.	[24]
3	Strawberry seed extract	XRD, UV/Vis, SEM, DLS, EDX, FTIR	Exhibited a spherical shape with a particle size range of 50–70 nm, demonstrated antioxidant potential (DPPH, ABTS), and showed broad-spectrum antibacterial activity against both gram-positive and gram-negative strains, including *E. coli*, *S. typhimurium*, *S. sonnei*, *H. halophila*, *S. aureus* and *B. subtilis*.	[25]
4	*D. lotus* leaf extracts	UV-Vis, EDX, XRD and SEM	Featured a face-centered cubic arrangement with an average size of about 27 nm and exhibited effective photocatalytic performance toward industrial wastewater.	[26]
5	*A. sativum* extracts.		Showed notable antioxidant capacity (TPC, TFC), exhibited antibacterial effects against *B. subtilis*, *S. aureus*, *E. coli*, and *P. multocida*, displayed anti-mutagenic activity in *S. typhimurium* TA98 and TA100, produced a dose-dependent response in the brine shrimp lethality test, and demonstrated in vitro anti-proliferative action against HepG2 cells.	[27]
6	*H. integrifolia* leave s extract	FTIR, FESEM, EDX, UV–vis	Exhibited a face-centered cubic structure with spherical particles measuring 32–38 nm, and showed strong bioactivity including antioxidant effects (DPPH, metal chelation, nitric oxide), along with anti-diabetic, anti-inflammatory, and antibacterial properties.	[28]
7	*T. indica* fruit extract	SEM, TEM, XRD, FT-IR, EDX	Displayed a face-centered cubic structure with an average size of around 10 nm and demonstrated pronounced antibacterial activity.	[29]
8	Eggshell membrane and *O. vulgare*	UV–Vis, TEM	Showed promising antibacterial activity	[30]
9	*J. auriculatum* ste m extracts	FT-IR, XRD, SEM, UV-Vis, EDX	Showed promising antibacterial activity	[31]
10	*O. vulgare* extract	UV-vis, FT-IR, XRD, *TEM and EDX*	Possessed a crystalline face-centered cubic structure with polydisperse nanoparticles averaging about 12 nm, and exhibited antimicrobial activity against *Shigella sonnei*, *Micrococcus luteus*, *E. coli*, *Aspergillus flavus*, *Alternaria alternata*, *Paecilomyces variotii*, and *Phialophora alba*.	[32]
11	*C. formosum, P. lanceolata, S. parasitica, C. minus, M. birdwoodiana, M. Africana, L. strychnifolia* extract	UV–Vis, TEM, ICP-OES	The biosynthesized AgNP formulations with average particle sizes as follows: AgNPs-1 (8.8 ± 0.3 nm), AgNPs-4 (17.7 ± 0.3 nm), AgNPs-5 (26.2 ± 0.7 nm), AgNPs-7 (16.4 ± 0.3 nm), AgNPs-12 (35.4 ± 5.9 nm), AgNPs-13 (11.4 ± 0.1 nm), and AgNPs-28 (15.7 ± 1.2 nm). Showed a spherical morphology with strong colloidal stability, exhibited antioxidant potential (DPPH, reducing power), demonstrated cytotoxic effects toward A549 lung cancer cells, and promoted wound-healing activity in NIH3T3 fibroblast cells.	[33]
12	*Trapa natans* leaf extract	FTIR, XRD, SEM,	Had particle dimensions between 30 and 90 nm and exhibited notable anticancer effects against A431 skin carcinoma cells.	[34]
13	*S. cayennensis* extr act	UV-Vis, IR, PXRD, SEM, EDX	Showed crystallite sizes of approximately 13 nm and 20 nm, along with measurable antioxidant activity (H_2O_2 scavenging, phosphomolybdenum assay) and anti-inflammatory potential evaluated through the egg albumin denaturation test.	[35]
14	*S. bryopteris* extract	PXRD,UV-Vis., FESEM, TE M and EDX.	Demonstrated broad antimicrobial efficacy against bacterial and fungal strains, along with noticeable anti-coagulant and anti-platelet activities.	[36]
15	Linseed aqueous extract	FTIR, XRD, SEM, UV-Vis,	Displayed a spherical morphology with an average diameter of about 34.47 nm, showed antibacterial and anti-biofilm effects against *E. coli* and *B. subtilis*, and exhibited antioxidant potential as indicated by DPPH, TPC, and TFC analyses.	[37]
16	*Litchi chinensis peel extract*	XRD, SEM, FTIR	FFC, average particle size 18.15 nm, semi-spherical particle, exhibited promising antimicrobial and antioxidant, biocompatible and non-toxic	Present study

Experimental

Reagents and Chemicals

Folin-Ciocalteu reagent, gallic acid, catechin, $AgNO_3$ and synthetic free radical (DPPH) were purchased from Sigma-Aldrich, USA. Fetal Bovine Serum along with DMEM medium was procured from Thermo-Fisher. Nutrient agar was purchased from Oxide (UK). Ethanol, methanol, sodium hydroxide, Vogel media, glucose, sodium nitrate, sodium carbonate, ferrous chloride, potassium dichromate, aluminum chloride, sodium azide, ammonium thiocyanate, cis-platin and tetrazolium compound for MTT were procured from Merck, Germany. The ciprofloxacin was purchased from medicine market.

Sample collection and its preparation

Fresh fruits of *Litchi chinensis* were collected from the local market of district Jhang and further authenticated by the Taxonomist Ms. Zahira Rafique, Lecturer, Department of Basic Sciences (Section Botany), UVAS (Jhang Campus), Pakistan. Then the fruits were rinsed with double distilled water, then disinfected with sodium dichloroisocyanurate and separated into peel, pulp and seed. Peels were shade-dried at room temperature for 20 days [38]. These dried peels were ground into fine powder (80 mesh), which was stored at -4 °C in an airtight glass jar for further analyses.

Preparation of LCP aqueous extract

The bioactive components from LCP were extracted using maceration [39]. Briefly, dry powder (30 g) was mixed with distilled water (100 mL) using an orbital shaker (220 rpm) at room temperature for 48 hours and subsequently filtered to separate insoluble residue. The collected filtrate was collected and lyophilized to obtain a dried powder of aqueous LCP extract, which was stored at -4°C.

Preparation of AgNPs

The AgNPs were prepared using LCP aqueous extract following the method [40]. Briefly, an aqueous solution of $AgNO_3$ (0.2M) was mixed with LCP aqueous extract at a fixed ratio of 4:1 (v/v), heated at 60 °C with stirring for 10 min. Bioactive components of LCP facilitated to reduction of silver ions Ag^+ (yellowish) to Ag (reddish brown) [41]. The resultant mixture was processed for centrifugation (5000 rpm) and successive washing with deionized water and ethanol. The prepared LCP-AgNPs were lyophilized to analysis. The reduction and stabilization of nanoparticles were confirmed using various characterization techniques.

Antioxidant activity

The antioxidant activity of LCP and LCP-AgNPs was performed by estimating the TPC, TFC and scavenging potential (DPPH) in a 50-200 mg/mL concentration range.

Estimation of TPC

Folin-Ciocalteu (FC) regent-based method was employed to estimate the phenolic contents present in LCP aqueous extract and LCP-AgNPs [42]. Briefly, each stock solution (300 µL) was mixed with FC reagent (2M, 500 µL) and sodium carbonate (Na_2CO_3) solution (800 mM, 1 mL) in separate glass test tubes followed by homogenization. Following a 2-hour incubation at room temperature, the absorbance of each sample was measured at 765 nm. Total phenolic content was then calculated and reported as gallic acid equivalents (GAE) per gram of dry extract.

Quantification of TFC

TFC of each LCP aqueous extract and LCP-AgNPs was determined following the reported method [43]. Briefly, each stock solution (1 mL) was mixed with sodium nitrate solution (5%, 400 µL) and the resultant mixture was diluted with distilled water (6 mL). After incubating the resultant mixture for 5 min, Al_2Cl_3 solution (10%, 700 µL) and NaOH solution (1 M, 3 mL) were added successively. The absorbance of the reaction mixture was measured at 510 nm. The concentration of TFC of each solution was expressed as catechin equivalent (CE) per g DW of extract.

DPPH scavenging assay

The reducing capacity of all prepared stock solutions of both samples was assessed against a stable free radical DPPH. DPPH solution (0.004% methanolic solution, 180 µL) was mixed with each stock solution (1mL) and incubated in the dark for 1 hr. The absorbance of the final reaction mixture was measured at 517nm and the radical scavenging effect (% inhibition) was calculated by using the relation shown in Eq. 1 (where A_b and A_s are the absorbance values of blank and sample, respectively). This assay was performed in triplicate by using ascorbic acid as a standard [44].

$$\text{Scavenging effect (\%)} = \frac{A_b - A_s}{A_b} \times 100 \qquad (1)$$

Antibacterial activity analysis

Four bacterial strains were employed to evaluate the bactericidal potential of LCP aqueous extract and LCP-AgNPs by agar well diffusion assay [45]. Briefly, different concentrations (50, 100, 150, 200 mg/mL) of stock solutions of LCP aqueous extract and LCP-AgNPs were prepared. Bacterial strains fresh cultures were grown in nutrient broth at 37 °C. Freshly grown bacterial culture (100 µL) was spread over sterilized nutrient agar in petri plates, following incubation at room temperature for 20 minutes. For antibacterial activity, each stock solution (50 µL) was loaded in the wells of 7 mm on each agar plate, followed by incubation at 37 °C for 14 h. Ciprofloxacin was used as a positive control at a

concentration of 1mg/mL per well under similar experimental conditions. The zone of inhibition (mm) were recorded using a zone reader.

XRD analysis

Crystallographic analysis of synthesized AgNPs capped with bioactive compounds of *Litchi chinensis* peels was evaluated using a powder XRD Diffractometer (Model D2 Phaser XE-T Edition). Briefly, the LCP-AgNPs powder was diluted with methanol and ground to get a fine mixture (grain size of about 1 µm). Then, the sample mixture (3 µL) was loaded over the copper-coated grid as a thin film, and the additional sample was removed using blotting paper. XRD analysis was performed by directing the X-rays (λ= 1.5406 Å) over nanomaterials [46]. Incident X-rays interacted with the sample and produced a diffracted ray pattern in the spectrum, which was recorded at specific intensities with 2θ values ranging from 30-90º. OriginPro software was used to interpret the observed XRD spectrum.

Surface morphology analysis

Surface morphology and particle size analysis of LCP aqueous extract and LCP-AgNPs was evaluated by performing SEM analysis following a reported method [47] with minor modifications. Both samples were prepared with the help of ultrasonic waves at 37 ºC for 15 min. These samples (5 µL each) were coated with gold and surface morphology was recorded using SEM (Modal-FEI Nova 450 NanoSEM) at a resolution power of 10 nm. High-energy electrons from the source interacted with bioactive components of both samples and images were produced by scanning at an accelerating voltage of 10 kV. ImageJ software was used to calculate the size distribution histogram.

FTIR analysis

The potassium bromide (KBr) pellet method was employed for structural and functional group analysis of the LCP aqueous extract and LCP-AgNPs following a reported protocol [48] with minor modifications. Briefly, 3 mg of each sample was homogenized with dry KBr powder, and the resulting transparent pellet was exposed to infrared (IR) radiation (10,000–100 cm^{-1}) to record the spectra. The FTIR analysis was performed in the frequency range of 4000–500 cm^{-1}, and the spectra were obtained as percent transmittance using an FTIR spectrometer (Model: Bruker Alpha Platinum ATR) equipped with an Intron Infrared Microscope.

Cell viability (MTT) assay

A freshly prepared HepG2 cell culture was utilized for the cell viability assessment [49]. The HepG2 liver cancer cell line (RRID: CVCL_0027) was sourced from ATCC (Manassas, VA, USA; catalog no. HB-8065). Cells were maintained under sterile conditions in Dulbecco's Modified Eagle Medium (DMEM) enriched with 10% fetal bovine serum and 1% penicillin–streptomycin, and incubated at 37 °C in a humidified atmosphere containing 5% CO_2. After 24 hours, cell growth and morphology were examined under an inverted microscope. In 96-well plates with a flat bottom, cells were planted at a concentration of 5×10^4 cells/well. After incubation of 16 h, 50 µL of four different concentrations (50 -200 mg/mL) of LCP aqueous extract and LCP-AgNPs were poured separately into each well. Similarly, negative control (growth media with HepG2 cells) and positive control of cisplatin (5 µL/well) were also processed under similar experimental conditions. After 48 h, the medium was replaced with the new medium containing MTT reagent. After 4 h of incubation, HepG2 Cell viability was recorded by the reduction of tetrazolium compound MTT (3-[4, 5-dimethylthiazol-2-yl]-2,5-diphenyltetrazolium bromide) into an insoluble purple color formazan by a metabolically active mitochondrial enzyme. An ELISA (Enzyme-Linked Immunosorbent Assay) plate reader was used for absorbance measurement (extend of cell survival) at 570 nm and viable cells (%) were calculated using Eq. 2.

$$\text{Cell viability (\%)} = \frac{OD_{sample} - OD_{Blank}}{OD_{Control} - OD_{Blank}} \qquad (2)$$

where OD_{sample} and $OD_{control}$ were the absorbance values of LCP samples and positive control cells (Cisplatin), respectively. OD_{blank} was the absorbance of negative control cells at 570 nm. Each experiment was performed in triplicate, and the data are presented as the mean ± standard deviation [50].

Mutagenicity assay

Mutant bacterial strains *S. tyhimurium* TA98 and TA100 were treated with four different concentrations (50 to 200 mg/mL) of aqueous LCP extract and green synthesis using AgNPs to investigate their mutagenicity using the Ames test [51, 52]. Briefly, fresh cultures of bacterial strains were prepared in nutrient broth at 35 ºC followed by incubation overnight and then stored at -80ºC as frozen stock cultures till analyzed. For mutagenic assessment, molten agar (2 mL) was mixed with 100 µL of each

concentration of LCP aqueous extract and LCP-AgNPs following the addition of prepared culture (100 µL) and incubated at room temperature for 20-30 min. The resultant mixture of each concentration was poured into separate petri plates containing 20 mL of minimal agar. Distilled water was used as a blank, while $K_2Cr_2O_7$ and NaN_3 were used as a positive control against the TA98 and TA100 strain, respectively. After solidification of media (15-20 min), the plates were inverted and incubated at 37 ºC for 24-48 h. The revertant colonies were then counted using an automated colony counter.

Statistical analysis

Results of all assays of aqueous LCP aqueous extract and LCP-AgNPs were expressed as means ± standard deviation [53].

Results and Discussion

Structural properties

Incident electromagnetic rays (X-rays) were scattered over crystal atoms of AgNPs and produced X-ray diffraction patterns, which define and confirm the crystallographic structure of AgNPs bound to bioactive compounds in LCP [54]. The resulting XRD patterns are depicted in Fig. 1. Five distinct diffraction peaks were indexed at (1 1 1), (2 0 0), (2 2 0), (3 1 1) and (4 2 2) with corresponding 2Θ angles of 38.16º, 46.63º, 63.22º, 78.72º and 83.79º, respectively. While only three distinct peaks indexed at 2Θ angles of 38.31º, 44.44º, and 64º, were observed by Arif et. al. during XRD analysis of AgNPs synthesized from LCP and marked only one peak corresponding to (1 1 1) for the confirmation of nanoparticles synthesis. In comparison, recent XRD spectrum and peak calculations suggested the predominant growth of AgNPs along (2 0 0), (2 2 0) and (3 1 1), which was also confirmed by literature [23]. Moreover, the obtained data was matched with the standard data of JCPDS file No. 03092 and reported. The average crystalline size and lattice planes of all the observed peaks were calculated and presented in Table 2. Using the Debye-Scherrer equation, the average crystalline size of AgNPs was calculated to be 18.15 nm. Sharp, intense peaks were the representation of the crystalline nature of AgNPs. Secondary peaks have also been observed, which are due to phytochemicals present in LCP capped with silver nanoparticles [55]. Specific orientations of crystallites at the 2θ angle confirm silver's face-centered cubic structure. Lattice plane values indicated the green synthesis of AgNPs.

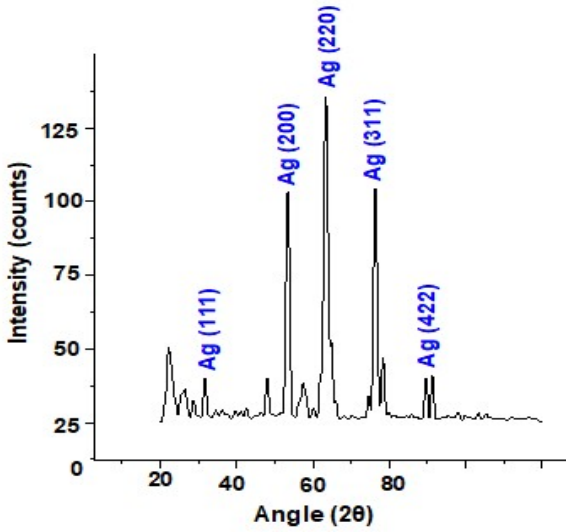

Fig. 1: XRD pattern of AgNPs prepared using *L. chinensis* peels aqueous extract.

Table-2: Structural parameters of AgNPs prepared using *L. chinensis* peels aqueous extract.

Peak No	Peak position (2θ)	FWHM (β)	Crystallite size nm	d-spacing (Å)	Lattice planes (hkl)
1	38.16	0.54	15.56	2.35	1 1 1
2	46.63	0.36	24.02	1.94	2 0 0
3	63.22	0.86	10.84	1.46	2 2 0
4	78.72	0.84	12.23	1.21	3 1 1
5	83.79	0.38	28.08	1.15	2 2

Surface morphology analysis

The SEM analysis was performed of both AgNPs and the extracts and the responses are depicted in Fig. 2. Surface morphology of both samples could easily be distinguished. The morphology of the LCP extract showed a uniform surface (Fig. 2A). A semi-spherical particle with a tendency to aggregate formation was observed in SEM analysis, which is attributed to interactions between biomolecules on the particle surface. The particles are distributed unevenly, which is due to the agglomeration formation of the nanoparticles, which is due to the presence of bioactive molecules on the surface and these biomolecules induced attractive interactions among themselves (Fig. 2B). The particle size distribution of AgNPs using ImageJ software revealed an average particle size of 25.56 nm. The surface morphology is comparable to the previous findings [56].

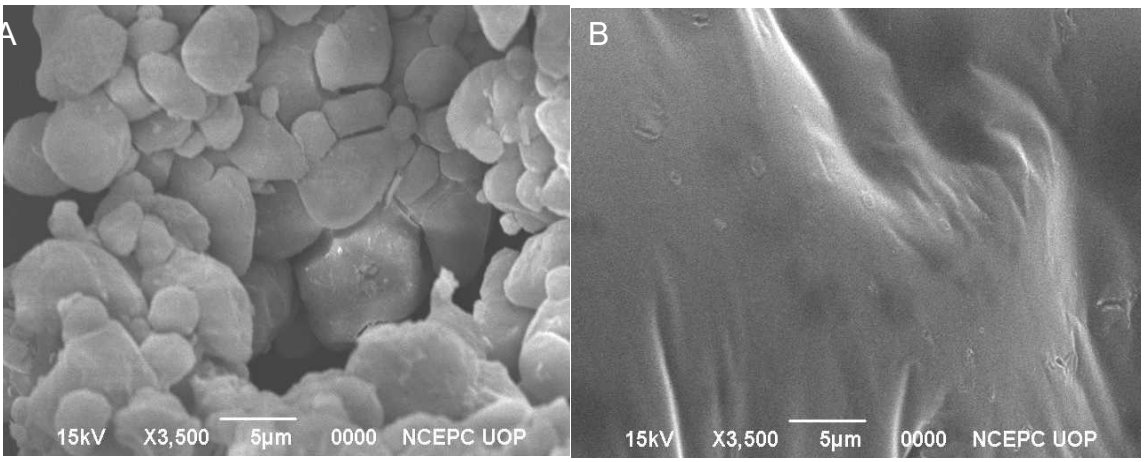

Fig. 2: Surface morphology of (A) *Litchi chinensis* peels aqueous extract and (B) *Litchi chinensis* peels-based AgNPs.

FTIR analysis

FTIR analysis confirmed the bioreduction of silver ions (Ag^+) to AgNPs, which was ascribed to the occurrence of natural bioactive compounds present in LCP aqueous extract. This phenomenon was exhibited by spectral patterns linked with specific functional groups (Fig. 3). Aqueous LCP extract (Fig. 3A) displayed a broad absorption band in the functional group region at 3315.02 cm^{-1} representing the O-H stretching vibrations of polyols such as catechin and hydroxyflavones, which confirmed the presence of caffeic acid, tannic acid, and reversterol [57, 58]. The appearance of a sharp absorption band at 1636.36 cm^{-1} corresponds to bending vibrations of C-H bonds of aromatic compounds, respectively [59]. These findings were comparable to the results of FTIR analysis by Singh et. al [60] where *litchi chinensis* peels were used against the inhibition of corrosion of mild steel [60]. Similarly, FTIR analysis of LCP silver nanoparticles gives IR absorption bands located at the wavelength range of 1636.36-728.50 cm^{-1} as indicated in Fig. 3B. The occurrence of the sharp intense peak at 1633.54 cm^{-1} was associated with C=C stretching vibration of disubstituted Cis-alkenes. These compounds were formed as oxidized products on subsequent reduction of Ag^+ ions [61]. Stretching vibrations of –C-C- bonds of aromatic compounds showed an absorption band at 1416.06 cm^{-1} and free hydroxyl groups on aromatic rings were considered as stabilizing agents for silver nanoparticle synthesis [62]. In the fingerprint region, an intense absorption peak at 1311.23 cm^{-1} was linked to –C-O stretching frequencies, indicating the presence of alcohols, carboxylic acids, esters and ethers [63]. The appearance of absorption peaks at 1051.18 cm^{-1} and 805.82 cm^{-1} was due to the C-N stretching frequency of aliphatic amines and the C-H (out of plan) blended frequency of aromatics [64]. Similar absorption bands were also observed by Azmath et al. [65] for AgNPs synthesized using *Endophytic colletotrichum* sp., where the absorption bands represented the presence of a maximum number of biomolecules for the stabilization of nanoparticles. Although previous studies also analyzed the FTIR spectral pattern of AgNPs synthesized from LCP [66], it was not well explained. Based on our research, it is suggested that the above-mentioned bioactive components be separated from the LCP aqueous extract and utilized in the synthesis of silver nanoparticles for use in medicines.

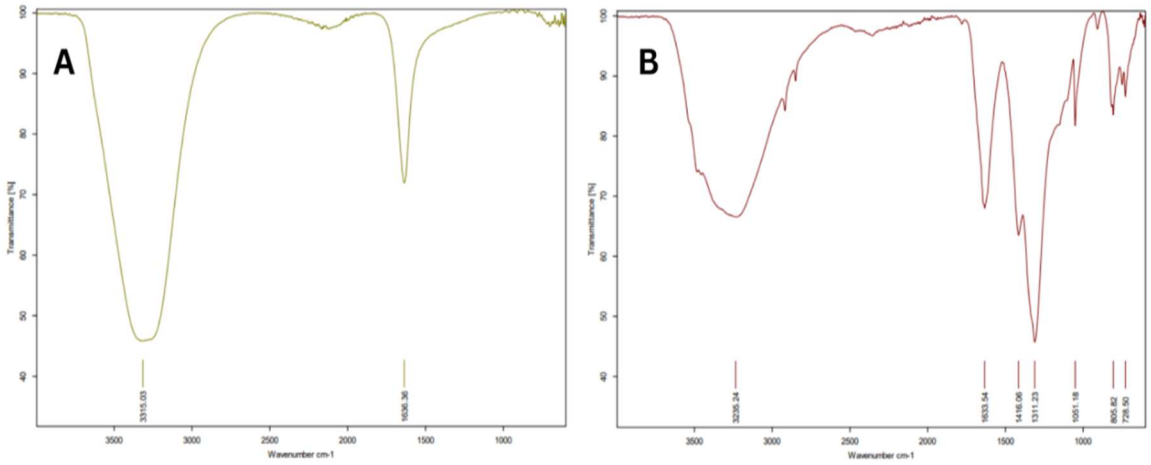

Fig. 3: FTIR spectral pattern of (A) *Litchi chinensis* peels aqueous extract and (B) *Litchi chinensis* peels AgNPs.

Antioxidant activity

TPC and TFC analysis

Phenolics and flavonoids possess strong pharmacological and biochemical potential, and their abundant presence plays a key role in facilitating the bioreduction of silver ions as well as stabilizing the resulting AgNPs [67]. Table 3 depicts a linear relationship between phenolic content and concentration of LCP extracts. Phenolic content was significantly increased when silver ions were used as a vehicle for bioactive compounds of LCP. TPC of various concentrations (50, 100, 150, and 200 mg/mL) of LCP aqueous extract was evaluated to be 13.46, 19.37, 26.65 and 38.21 mg GAE/g DW, respectively. The wide range of structural features found in plant polyphenols allows them to function effectively as reducing agents, hydrogen donors, and quenchers of singlet oxygen. On the other hand, LCP-AgNPs showed significantly higher phenolic activities, i.e., 17.21, 25.28, 36.31 and 48.46 mg GAE/g DW using stock solutions over the concentration range of 50-200 mg/mL. These findings are in line with those of the literature [47], where AgNPs were found to increase the antioxidant potential of phytochemicals in the tested extract. Quantitative evaluation of flavonoid components in both samples is depicted in Table 3. TFC of any sample is based on the solvents used for extraction and polar solvents are the most favorable for flavonoid extraction [68]. A significantly higher antioxidant potential was exhibited by LCP-AgNPs compared to aqueous extract over the range of concentrations used. The comparison of the maximum TFC of LCP aqueous extract and LCP-AgNPs was determined to be 26.93 and 35.83 mg CE/g DW, respectively, at the concentration of 200 mg/mL. The minimum TFC was determined to be 9.21 and 13.67 mg CE/g DW, respectively, at 50 mg/mL. It was observed that TFC has a direct relationship with the concentration of LCP aqueous extract/AgNPs. The results of the present investigation were in line with the reported study [69], where a study was conducted to evaluate the bioactive constituents of LCP extract based on their m/z values. The extracted compounds were mainly catechins and anthocyanins, where Cyanindin-3-*O*-rutiside was the major flavonoid. Catechins and anthocyanins have been reported to express anti-cancer, anti-inflammatory and antioxidant properties [69].

DPPH Scavenging assay

Evaluation of free radical scavenging activity of LCP aqueous extract and LCP-AgNPs against standard stable free radical (DPPH) revealed that as we increased the concentration of aqueous extract from 50 mg/mL to 200 mg/mL, scavenging potential (% inhibition) was gradually increased from 28.26 to 73.36 %, respectively. Progressively increasing scavenging potential was observed for a 50-200 mg/mL concentration range of LCP-AgNPs, which was evaluated to be 35.42, 48.25, 61.43, and 84.93 (%), respectively. The excellent scavenging potential of silver nanoparticles was due to the presence of phytoconstituents (capping agents) of LCP [66]. This fact was confirmed by the higher flavonoid and phenolic content of green-synthesized AgNPs from our study. The maximum number of phytochemicals are responsible for the bioreduction of AgNPs (Table 3), which was in line with the literature [70]. The reported major phytoconstituents present in LCP were found to be catechins, anthocyanins, and hydroxyflavones [69].

Table-3: Antioxidant activity assessment of LCP aqueous extract and LCP-AgNPs by TPC, TFC and DPPH scavenging assay

Sr. No.	*Sample*	Concentration (mg/mL)	Antioxidant activity		
			TPC (mg GAE/g DW)	TFC (mg CE/g DW)	DPPH (% inhibition)
1.		50	13.46 ± 1.2	09.21 ± 1.4	28.26 ± 1.5
2.		100	19.37 ± 2.5	16.63 ± 3.1	44.64 ± 1.8
3.	*Litchi chinensis* aqueous extract	150	26.65 ± 3.6	20.47 ± 1.3	56.29 ± 1.4
4.		200	38.21 ± 1.2	26.93 ± 2.7	73.36 ± 2.6
5.		50	17.21 ± 3.8	13.67 ± 2.3	35.42 ± 1.3
6.	*Litchi chinensis* AgNPs	100	25.28 ± 1.7	19.83 ± 3.1	48.25 ± 1.6
7.		150	36.31 ± 2.6	24.37 ± 1.3	61.43 ± 0.5
8.		200	48.46 ± 2.8	35.83 ± 3.7	84.93 ± 1.0

Values represent the mean ± SD for three replicates (n = 3)
GAE refers to gallic acid equivalents (mg/g dry weight of extract)
CE denotes catechin equivalents (mg/g dry weight of extract)

Antibacterial potential

The antibacterial potential of the LCP aqueous extract and LCP-AgNPs was assessed against selected Gram-positive and Gram-negative bacteria using the agar well diffusion method. Both materials produced distinct inhibition zones, and the diameter of these zones increased with increasing sample concentrations (Table 4). Ciprofloxacin showed the highest antibacterial activity against all tested bacterial strains. LCP-AgNPs (200 mg/mL) exhibited maximum inhibition against *S. aureus* (38 mm), *B. subtilis* (36 mm), followed by *P. multocida* (25 mm) and *E. coli* (23 mm). The LCP aqueous extract displayed significantly lower antibacterial activity compared to LCP-AgNPs at all concentrations. The excellent antibacterial activity of LCP-AgNPs lies in the fact that the nanosize nature of phytochemical-based metal particles enables them to harm the cell membrane of pathogenic bacteria, which results in the destabilization of the membrane by binding to phosphorylated proteins and consequently microbial inactivation occurs [74]. The antibacterial potential of AgNPs capped with *Calotropis pocera* latex against gram-positive strains was significantly higher than that of gram-negative strains [53]. The antibacterial activity of green-synthesized AgNPs was enhanced when combined with LCP aqueous extract showing its synergistic effect [66]. This dose-dependent antibiobacterial potential of LCP-AgNPs against both gram-positive and negative bacterial strains suggests their use against various bacterial infections and inflammatory diseases. The small size range of nanoparticles between 5.52 and 24.65 nm, recorded by SEM, confirmed their greater versatility in combating intracellular bacteria [71].

Cytotoxicity studies

The biocompatibility of the aqueous extract and LCP-AgNPs at four different concentrations was examined using the MTT assay on HepG2 cells, and the results were compiled in Table 5. Both samples showed comparable levels of cell viability, with no notable differences between them. This study provides the first comparative evaluation of the anticancer response of LCP-derived silver nanoparticles and the corresponding aqueous extract against the HepG2 cell line. The findings of this analysis revealed that treatment of HepG2 cells with aqueous extract and LCP silver particles for 48 h considerably decreased cell numbers. Maximum anticancer potential of aqueous and silver particles extract of LCP shows cell viability 58.42 at 200 mg/mL concentration in aqueous extract and while, using silver particles as a carrier of different bioactive compounds across the cell membrane and inhabit the replication pathway in HepG2 cell, cell viability reduce, 43.52 at the same concentration (200 mg/mL) concentration in LCP silver particle, significant increase in its anticancer activity due to silver particle provide a vehicle service for the transport of active constituents in LCP extract across the HepG2 cell used in current study. When the concentration of extract was decreased, the cell viability was enhanced and showing less anticancer potential; its mean anticancer activity is concentration dependent. A similar trend of decreasing cell viability with the increase of concentration of tested compounds was observed [72]. Phenolic and flavonoid constituents of LCP extract have anticancer and anti-inflammatory properties [69]. Our study reveals that LCP silver particles have excellent scavenging potential at various concentrations. The evaluation of the methanolic extract of various fruits against the MCF-7 cell line revealed that phytoconstituents exhibited the ability to increase tumor vascularization and metastasis [67]. The excellent cytotoxic potential of LCP silver particles were associated with their enhanced triggering action of ROS production, which caused cell death and cellular uptake by pinocytosis and endocytosis [67].

The values indicate the inhibition zone (mm) produced by each concentration of the LCP extracts against the tested bacterial strains and are presented as mean ± SD for three replicates (n = 3). Rifampicin served as the positive control for all four bacterial species.

The values represent the relative number of viable cells, determined by the ELIZA plate reader and are the mean± S.D of triplicate samples (n = 3), blank (without any extract) and cis-platin was a positive control (5 µL/mL).

Table-4: Antibacterial activity of LCP aqueous extract and LCP-AgNPs.

Sr. No.	Sample	Concentration (mg/mL)	Zone of inhibition (mm)			
			E. coli	*B. subtilis*	*P. multocida*	*S. aureus*
1.	LCP aqueous extract	50	09±1.4	18±0.6	11±1.7	20±1.4
2.		100	13±1.5	23±1.3	17±2.3	25±0.9
3.		150	16±0.8	29±2.7	20±1.6	30±0.7
4.		200	21±1.6	34±2.4	24±2.5	35±0.6
5.	LCP-AgNPs	50	10±0.7	19±1.8	12±0.8	22±1.5
6.		100	14±1.5	26±1.2	19±1.3	27±1.4
7.		150	18±0.6	32±0.5	22±1.5	31±1.5
8.		200	23±1.5	36±1.17	25±1.4	38±1.8
9.	Positive control	10	37±1.7	41±1.6	39±1.5	42±0.8

Table-5: Cytotoxic evaluation of aqueous extract and LCP silver particles against the HepG2 cell line.

Sr. No.	Sample	Concentration (mg/mL)	Cell Viability
1.	*Litchi chinensis* aqueous extract	50	89.64±6.32
2.		100	76.34±12.83
3.		150	67.79±6.40
4.		200	58.42±14.53
5.	*Litchi chinensis* AgNPs	50	78.41±12.64
6.		100	66.37±8.63
7.		150	57.29±6.38
8.		200	43.52±10.57
9.	Negative control	without extract	91.46±16.58
10.	Positive Control	5 µl/mL	15.23±3.40

Mutagenic studies

Mutagenicity evaluation of four concentrations of LCP aqueous extract and LCP-AgNPs was performed for the first time against two mutant strains of *Salmonella tyhimurium* TA98 and TA100 and the results were presented in Table 6. According to the results of the present analysis, a high concentration of aqueous LCP aqueous extract and LCP-AgNPs induced a significant increase in revertant colonies compared to the positive control. The negative control showed no mutagenicity against the tested bacterial strains. LCP aqueous extract exhibited revertant colonies in the range of 551–689 and 658-814 against mutant strain TA98 and TA100, respectively. This behavior was attributed to the occurrence of phytochemicals such as polyols, aromatics, alkenes, alkanes, carboxylic acids, ethers, esters and aliphatic amines, found by FTIR analysis of LCP extract and LCP-AgNPs. A similar trend was also observed by treating with different concentrations of LCP AgNPs, where the maximum number of revertant colonies against both tested strains was proportional to their ascending concentration of extract. Similarly, Padilla-Camberos et al. [73] reported that green AgNPs did not have any mutagenic or genotoxic effects. The present study concluded that all tested concentrations of the aqueous LCP extract and LCP-AgNPs exhibited no mutagenic or toxic effects, as the number of revertant colonies did not exceed that of the control.

Comparative analysis

The comparison of the previous reports on green-synthesised AgNPs is depicted in Table 1. The studies show significant differences in reducing agents, nanoparticle size and biological activity. Numerous studies, including those that use *A. Cepa* [8], *S. mollis* [24] and strawberry seed extract [25] generated particles with potent antibacterial or antioxidant qualities that ranged in size from 50 to 85 nm. Studies using *T. indica* fruit extract produced very small AgNPs [29]. The lotus leaf extracts lotus-based AgNPs [26] demonstrated both photocatalytic and antibacterial properties. Similarly, extracts like *A. sativum* [27], *H. integrifolia* [28], as well as S. *Cayennensis* [35] produced nanoparticles with additional biological properties, such as anti-diabetic, anti-inflammatory and anti-mutagenic properties. Many of these systems lacked combined multifunctionality, biocompatibility, and eco-friendly precursor utilization in a single platform, despite the fact that several reports showed broad-spectrum antimicrobial behavior [30–32] or specialized bioactivities like wound healing [33], anticancer efficacy [34] or anticoagulant effects [36]. On the other hand, in the current study the peel extract from *Litchi chinensis* shows several advantages. The furnished AgNPs had a semi-spherical FFC crystalline nature and were smaller (average particle size 18.15 nm) than many formulations that had been previously published. The process was more sustainable than many previous plant-based systems because litchi peel, a waste product has high polyphenols, found to be efficient for reducing and stabilizing the Ag NPs. The resultant NPs demonstrated concurrent antimicrobial, antioxidant, cytocompatible and non-toxic nature a multifunctional profile that was uncommonly seen in earlier research. Compared to previously published AgNPs, the current system is a better option for biomedical and environmental applications due to its waste valorization, environmentally friendly synthesis, biocompatibility and broad bioactivity.

Table-6: *In vitro* mutagenicity or genotoxicity of LCP extract and LCP-AgNPs against Mutant strains of *S. typhimurium* TA98 and TA100.

Sr. No.	Sample	Concentration (mg/mL)	*S. typhimurium* TA98	*S. typhimurium* TA100
1.		50	[a] 551±84	[a] 658±103
2.		100	597±103	706±156
3.	LCP aqueous extract	150	631±56	736±103
4.		200	689±79	814±154
5.	LCP-	50	536±161	617±203
6.	AgNPs	100	563±89	664±58
7.		150	589±106	704±62
8.		200	615±149	749±135
9.	[b] Negative control	without extract	506±86	564±103
10.	[c] Potassium dichromate ($K_2Cr_2O_7$)	05	3326±125	-
11.	[c] Sodium azide (NaN_3)	05	-	4039±241

Mutant strains of *S. typhimurium* TA98 and TA100 were used. [a] The values represent revertant bacterial colonies, counted using an automated colony counter and are the mean± SD of triplicate samples (n=3), [b] Blank (without any extract) and [c] potassium dichromate ($K_2Cr_2O_7$) and sodium azide(NaN_3) were used as positive control against TA98 and TA100, respectively.

Conclusions

In this study, silver nanoparticles were successfully synthesized using the aqueous extract of *Litchi chinensis* peels, where the naturally occurring polyphenolic compounds acted as efficient reducing and stabilizing agents. Characterization confirmed the effective incorporation of LCP-derived phytochemicals on the nanoparticle surface. The green-synthesized LCP-AgNPs demonstrated noteworthy antibacterial and antioxidant activities, indicating that the phytochemical-capped nanoparticles can function as a promising natural alternative to synthetic antimicrobial agents. According to cytotoxic analysis, LCP-AgNPs demonstrated strong anticancer potential against HepG2 cells. Cellular uptake resulted in decreased viability due to increased oxidative stress-mediated necrosis or apoptosis. Crucially, mutagenicity tests on *S. typhimurium* TA98 and TA100 strains revealed no genotoxic effects. The findings highlight the therapeutic potential of LCP-mediated AgNPs as environmentally benign and biocompatible options for upcoming medication development. Strong *in vitro* performance and possible synergy with chemotherapeutic agents underscore the need for thorough *in vivo* studies, especially with regard to their suitability for biomedical applications.

Acknowledgements

This research project was funded by the Deanship of Scientific Research, Princess Nourah bint Abdulrahman University, through the Program of Research Project Funding After Publication, grant No (44-PRFA-P-102).

References

1. A.S. Babar, S.A.S. Chatha, A.U. Haq, Innovative Synthesis of Fe Doped ZnO-Zeolite Composite for Advanced Applications, Journal of The Chemical Society of Pakistan, 47 (2025) 474.
2. R.H. Riyan, M.H. Efat, M.A. Arafath, M.S. Hossain, Fe3O4 Nanoparticles, Metal-Organic Framework of Zr and Cu, and their Composites: Synthesis, Characterization, and Photocatalytic Activity, Journal of the Chemical Society of Pakistan, 47 (2025) 487-496.
3. R. Nawaz, M.A. Jamal, B. Naseem, M. Munir, M. Iqbal, Lanthanum/Iron Oxide Nanocomposite for Photo-Ultrafast Removal of Methyl Orange Dye and Toxicity Evaluation, Journal of the Chemical Society of Pakistan, 47 (2025) 221-233.
4. R. Khursheed, K. Dua, S. Vishwas, M. Gulati, N.K. Jha, G.M. Aldhafeeri, F.G. Alanazi, B.H. Goh, G. Gupta, K.R. Paudel, Biomedical applications of metallic nanoparticles in cancer: Current status and future perspectives, Biomedicine & pharmacotherapy, 150 (2022) 112951.
5. A.H. Faraji, P. Wipf, Nanoparticles in cellular drug delivery, Bioorganic & medicinal chemistry, 17 (2009) 2950-2962.
6. T.-W. Yu, D. Anderson, Reactive oxygen species-induced DNA damage and its modification: a chemical investigation, Mutation Research/Fundamental and Molecular Mechanisms of Mutagenesis, 379 (1997) 201-210.
7. N.M. Salem, A.M. Awwad, Green synthesis and characterization of ZnO nanoparticles using Solanum rantonnetii leaves aqueous extract and antifungal activity evaluation, Chemistry International, 8 (2022) 12-17.
8. A. Naseer, M. Iqbal, S. Ali, A. Nazir, M. Abbas, N. Ahmad, Green synthesis of silver nanoparticles using Allium cepa extract and their antimicrobial activity evaluation, Chemistry International, 8 (2022) 89-94.
9. K. Chitra, A. Manikandan, S. Moortheswaran, K. Reena, S.A. Antony, Zingiber officinale extracted green synthesis of copper nanoparticles:

structural, morphological and antibacterial studies, Advanced Science, Engineering Medicine, 7 (2015) 710-716.
10. N. Kabeerdass, A. Al Otaibi, M. Rajendran, A. Manikandan, H.A. Kashmery, M.M. Rahman, P. Madhu, A. Khan, A.M. Asiri, M. Mathanmohun, Bacillus-mediated silver nanoparticle synthesis and Its antagonistic activity against bacterial and fungal pathogens, Antibiotics, 10 (2021) 1334.
11. F. Ali, G. Moin-ud-Din, M. Iqbal, A. Nazir, I. Altaf, N. Alwadai, U.H. Siddiqua, U. Younas, A. Ali, A. Kausar, Ag and Zn doped TiO2 nano-catalyst synthesis via a facile green route and their catalytic activity for the remediation of dyes, Journal of Materials Research Technology, 23 (2023) 3626-3637.
12. M.W. Amer, A.M. Awwad, Green synthesis of copper nanoparticles by *Citrus limon* fruits extract, characterization and antibacterial activity, Chemistry International, 7 (2021) 1-8.
13. A.M. Awwad, N.M. Salem, M.M. Aqarbeh, F.M. Abdulaziz, Green synthesis, characterization of silver sulfide nanoparticles and antibacterial activity evaluation, Chemistry International, 6 (2020) 42-48.
14. A. Alagarsamy, S. Chandrasekaran, A. Manikandan, Green synthesis and characterization studies of biogenic zirconium oxide (ZrO2) nanoparticles for adsorptive removal of methylene blue dye, Journal of Molecular Structure, 1247 (2022) 131275.
15. M. Dhayalan, M.I.J. Denison, M. Ayyar, N.N. Gandhi, K. Krishnan, B. Abdulhadi, Biogenic synthesis, characterization of gold and silver nanoparticles from Coleus forskohlii and their clinical importance, Journal of Photochemistry and Photobiology B: Biology, 183 (2018) 251-257.
16. A.M. Awwad, M.W. Amer, N.M. Salem, A.O. Abdeen, Green synthesis of zinc oxide nanoparticles (ZnO-NPs) using Ailanthus altissima fruit extracts and antibacterial activity, Chemistry International, 6 (2020) 151-159.
17. L.S. Al Banna, N.M. Salem, G.A. Jaleel, A.M. Awwad, Green synthesis of sulfur nanoparticles using Rosmarinus officinalis leaves extract and nematicidal activity against Meloidogyne javanica, Chemistry International, 6 (2020) 137-143.
18. O.U. Igwe, F. Nwamezie, Green synthesis of iron nanoparticles using flower extract of Piliostigma thonningii and antibacterial activity evaluation, Chem. Int, 4 (2018) 60-66.
19. V. Remya, V. Abitha, P. Rajput, A. Rane, A. Dutta, Silver nanoparticles green synthesis: a mini review, Chem. Int, 3 (2017) 165-171.
20. C.-C. Chyau, P.-T. Ko, C.-H. Chang, J.-L. Mau, Free and glycosidically bound aroma compounds in lychee (Litchi chinensis Sonn.), Food Chemistry, 80 (2003) 387-392.
21. M. Kanlayavattanakul, D. Ospondpant, U. Ruktanonchai, N. Lourith, Biological activity assessment and phenolic compounds characterization from the fruit pericarp of Litchi chinensis for cosmetic applications, Pharmaceutical Biology, 50 (2012) 1384-1390.
22. J. Li, Y. Jiang, Litchi flavonoids: isolation, identification and biological activity, Molecules, 12 (2007) 745-758.
23. A. Rautela, J. Rani, Green synthesis of silver nanoparticles from Tectona grandis seeds extract: characterization and mechanism of antimicrobial action on different microorganisms, Journal of Analytical Science and Technology, 10 (2019) 1-10.
24. A. Nazir, S. Farooq, M. Abbas, E.A. Alabbad, H. Albalawi, N. Alwadai, A.H. Almuqrin, M. Iqbal, Synthesis, characterization and photocatalytic application of Sophora mollis leaf extract mediated silver nanoparticles, Zeitschrift für Physikalische Chemie, 235 (2021) 1589-1607.
25. F. Ali, U. Younas, A. Nazir, F. Hassan, M. Iqbal, S. Mukhtar, A. Khalid, A. Ishfaq, Biosynthesis and characterization of silver nanoparticles using strawberry seed extract and evaluation of their antibacterial and antioxidant activities, Journal of Saudi Chemical Society, 26 (2022) 101558.
26. S. Yasmin, S. Nouren, H.N. Bhatti, D.N. Iqbal, S. Iftikhar, J. Majeed, R. Mustafa, N. Nisar, J. Nisar, A. Nazir, Green synthesis, characterization and photocatalytic applications of silver nanoparticles using Diospyros lotus, Green Processing and Synthesis, 9 (2020) 87-96.
27. M. Abbas, T. Hussain, J. Iqbal, A.U. Rehman, M.A. Zaman, K. Jilani, N. Masood, S.H. Al-Mijalli, M. Iqbal, A. Nazir, Synthesis of Silver Nanoparticle from Allium sativum as an Eco-Benign Agent for Biological Applications, Polish Journal of Environmental Studies, 31 (2022) 533-538.
28. V. Kumar, S. Singh, B. Srivastava, R. Bhadouria, R. Singh, Green synthesis of silver nanoparticles using leaf extract of Holoptelea integrifolia and preliminary investigation of its antioxidant, anti-inflammatory, antidiabetic and antibacterial activities, Journal of Environmental Chemical Engineering, 7 (2019) 103094.
29. N. Jayaprakash, J.J. Vijaya, K. Kaviyarasu, K. Kombaiah, L.J. Kennedy, R.J. Ramalingam, M.A. Munusamy, H.A. Al-Lohedan, Green synthesis of Ag nanoparticles using Tamarind fruit extract for the antibacterial studies, Journal of

Photochemistry and Photobiology B: Biology, 169 (2017) 178-185.
30. M. Baláž, N. Daneu, Ľ. Balážová, E. Dutková, Ľ. Tkáčiková, J. Briančin, M. Vargová, M. Balážová, A. Zorkovská, P. Baláž, Bio-mechanochemical synthesis of silver nanoparticles with antibacterial activity, Advanced Powder Technology, 28 (2017) 3307-3312.
31. S. Balasubramanian, U. Jeyapaul, S.M.J. Kala, Antibacterial activity of silver nanoparticles using Jasminum auriculatum stem extract, International Journal of Nanoscience, 18 (2019) 1850011.
32. M.R. Shaik, M. Khan, M. Kuniyil, A. Al-Warthan, H.Z. Alkhathlan, M.R.H. Siddiqui, J.P. Shaik, A. Ahamed, A. Mahmood, M. Khan, Plant-extract-assisted green synthesis of silver nanoparticles using Origanum vulgare L. extract and their microbicidal activities, Sustainability, 10 (2018) 913.
33. E.-Y. Ahn, H. Jin, Y. Park, Assessing the antioxidant, cytotoxic, apoptotic and wound healing properties of silver nanoparticles green-synthesized by plant extracts, Materials Science and Engineering: C, 101 (2019) 204-216.
34. M.M. Saber, S.B. Mirtajani, K. Karimzadeh, Green synthesis of silver nanoparticles using Trapa natans extract and their anticancer activity against A431 human skin cancer cells, Journal of Drug Delivery Science and Technology, 47 (2018) 375-379.
35. F.E.a. Meva, J.O.A. Mbeng, C.O. Ebongue, C. Schlüsener, Ü. Kökçam-Demir, A.A. Ntoumba, P.B.E. Kedi, E. Elanga, E.-R.N. Loudang, M.H.J. Nko'o, Stachytarpheta cayennensis aqueous extract, a new bioreactor towards silver nanoparticles for biomedical applications, Journal of Biomaterials Nanobiotechnology, 10 (2019) 102.
36. D. S.S, M. M.B, S.K. M.N, R. Golla, R.K. P, D. S, R. Hosamani, Antimicrobial, anticoagulant and antiplatelet activities of green synthesized silver nanoparticles using Selaginella (Sanjeevini) plant extract, International Journal of Biological Macromolecules, 131 (2019) 787-797.
37. M. Imran, S. Hussain, K. Mehmood, Z. Saeed, M. Parvaiz, U. Younas, H.A. Nadeem, S.P. Ghalani, S. Saleem, Optimization of ecofriendly synthesis of Ag nanoparticles by Linum usitatissimum hydrogel using response surface methodology and its biological applications, Materials Today Communications, 29 (2021) 102789.
38. A. Hussain, Sustainable production of silver nanoparticles from waste part of Litchi chinensis Sonn. and their antibacterial evaluation, Pakistan Journal of Pharmaceutical Sciences, 35 (2022) 85-94.
39. I.V. Rzhepakovsky, D.A. Areshidze, S.S. Avanesyan, W.D. Grimm, N.V. Filatova, A.V. Kalinin, S.G. Kochergin, M.A. Kozlova, V.P. Kurchenko, M.N. Sizonenko, Phytochemical characterization, antioxidant activity, and cytotoxicity of methanolic leaf extract of Chlorophytum Comosum (green type)(Thunb.) Jacq, Molecules, 27 (2022) 762.
40. H.F. Aritonang, H. Koleangan, A.D. Wuntu, Synthesis of silver nanoparticles using aqueous extract of medicinal plants'(Impatiens balsamina and Lantana camara) fresh leaves and analysis of antimicrobial activity, International journal of microbiology, 2019 (2019).
41. T. Mustapha, N. Misni, N.R. Ithnin, A.M. Daskum, N.Z. Unyah, A review on plants and microorganisms mediated synthesis of silver nanoparticles, role of plants metabolites and applications, International Journal of Environmental Research and Public Health, 19 (2022) 674.
42. M. Abbas, T. Hussain, M. Arshad, A.R. Ansari, A. Irshad, J. Nisar, F. Hussain, N. Masood, A. Nazir, M. Iqbal, Wound healing potential of curcumin cross-linked chitosan/polyvinyl alcohol, International Journal of Biological Macromolecules, 140 (2019) 871-876.
43. H.S. Salam, M.M. Tawfik, M.R. Elnagar, H.A. Mohammed, M.A. Zarka, N.S. Awad, Potential apoptotic activities of Hylocereus undatus peel and pulp extracts in MCF-7 and Caco-2 cancer cell lines, Plants, 11 (2022) 2192.
44. U. Sarker, S. Oba, S. Ercisli, A. Assouguem, A. Alotaibi, R. Ullah, Bioactive phytochemicals and quenching activity of radicals in selected drought-resistant Amaranthus tricolor vegetable amaranth, Antioxidants, 11 (2022) 578.
45. P. Junsathian, S. Nakamura, S. Katayama, S. Rawdkuen, Antioxidant and Antimicrobial Activities of Thai Edible Plant Extracts Prepared Using Different Extraction Techniques, Molecules, 27 (2022) 6489.
46. P.V. Kumar, S. Pammi, P. Kollu, K. Satyanarayana, U. Shameem, Green synthesis and characterization of silver nanoparticles using Boerhaavia diffusa plant extract and their anti bacterial activity, Industrial Crops and Products, 52 (2014) 562-566.
47. H. Zulfiqar, M.S. Amjad, A. Mehmood, G. Mustafa, Z. Binish, S. Khan, H. Arshad, J. Proćków, J.M. Pérez de la Lastra, Antibacterial, antioxidant, and phytotoxic potential of Phytosynthesized silver nanoparticles using

Elaeagnus umbellata fruit extract, Molecules, 27 (2022) 5847.
48. S.S. Alharthi, T. Gomathi, J.J. Joseph, J. Rakshavi, J.A.K. Florence, P.N. Sudha, G. Rajakumar, M. Thiruvengadam, Biological activities of chitosan-salicylaldehyde schiff base assisted silver nanoparticles, Journal of King Saud University-Science, 34 (2022) 102177.
49. M.M. Faheem, M. Bhagat, P. Sharma, R. Anand, Induction of p53 mediated mitochondrial apoptosis and cell cycle arrest in human breast cancer cells by plant mediated synthesis of silver nanoparticles from Bergenia ligulata (Whole plant), International Journal of Pharmaceutics, 619 (2022) 121710.
50. S. Chen, Y. Jiang, M. Fan, X. Zhang, Y. Zhang, T. Chen, C. Yang, W.-C. Law, Z. Xu, G. Xu, Highly biocompatible chlorin e6-poly (dopamine) core–shell nanoparticles for enhanced cancer phototherapy, Nanoscale Advances, 4 (2022) 4617-4627.
51. X. Guo, Y. Li, J. Yan, T. Ingle, M.Y. Jones, N. Mei, M.D. Boudreau, C.K. Cunningham, M. Abbas, A.M. Paredes, Size-and coating-dependent cytotoxicity and genotoxicity of silver nanoparticles evaluated using in vitro standard assays, Nanotoxicology, 10 (2016) 1373-1384.
52. D. Akyıl, Y. Eren, M. Konuk, H. Dere, A. Serteser, Genotoxic evaluation of Halfenprox using the human peripheral lymphocyte micronucleus assay and the Ames test, Drug and Chemical Toxicology, 40 (2017) 191-195.
53. Y. Wang, Y. Zhang, Y. Guo, J. Lu, V.P. Veeraraghavan, S.K. Mohan, C. Wang, X. Yu, Synthesis of Zinc oxide nanoparticles from Marsdenia tenacissima inhibits the cell proliferation and induces apoptosis in laryngeal cancer cells (Hep-2), Journal of Photochemistry and Photobiology B: Biology, 201 (2019) 111624.
54. M. Abbas, M. Arshad, M. Rafique, A. Altalhi, D. Saleh, M. Ayub, S. Sharif, M. Riaz, S. Alshawwa, N. Masood, Chitosan-polyvinyl alcohol membranes with improved antibacterial properties contained Calotropis procera extract as a robust wound healing agent, Arabian Journal of Chemistry, 15 (2022) 103766.
55. K. Anandalakshmi, J. Venugobal, V. Ramasamy, Characterization of silver nanoparticles by green synthesis method using Pedalium murex leaf extract and their antibacterial activity, Applied nanoscience, 6 (2016) 399-408.
56. S. Jebril, R.K.B. Jenana, C. Dridi, Green synthesis of silver nanoparticles using Melia azedarach leaf extract and their antifungal activities: In vitro and in vivo, Materials Chemistry and Physics, 248 (2020) 122898.
57. P. Wongsa, P. Phatikulrungsun, S. Prathumthong, FT-IR characteristics, phenolic profiles and inhibitory potential against digestive enzymes of 25 herbal infusions, Scientific Reports, 12 (2022) 6631.
58. T.K. Patle, K. Shrivas, R. Kurrey, S. Upadhyay, R. Jangde, R. Chauhan, Phytochemical screening and determination of phenolics and flavonoids in Dillenia pentagyna using UV–vis and FTIR spectroscopy, Spectrochimica Acta Part A: Molecular and Biomolecular Spectroscopy, 242 (2020) 118717.
59. S. Kainat, S.R. Gilani, F. Asad, M.Z. Khalid, W. Khalid, M.M.A.N. Ranjha, S.P. Bangar, J.M. Lorenzo, Determination and comparison of phytochemicals, phenolics, and flavonoids in Solanum lycopersicum using FTIR spectroscopy, Food Analytical Methods, 15 (2022) 2931-2939.
60. M.R. Singh, P. Gupta, K. Gupta, The litchi (Litchi Chinensis) peels extract as a potential green inhibitor in prevention of corrosion of mild steel in 0.5 M H2SO4 solution, Arabian Journal of Chemistry, 12 (2019) 1035-1041.
61. S. Rajeshkumar, L. Bharath, Mechanism of plant-mediated synthesis of silver nanoparticles–a review on biomolecules involved, characterisation and antibacterial activity, Chemico-biological interactions, 273 (2017) 219-227.
62. J. Jena, N. Pradhan, B.P. Dash, P.K. Panda, B.K. Mishra, Pigment mediated biogenic synthesis of silver nanoparticles using diatom Amphora sp. and its antimicrobial activity, Journal of Saudi Chemical Society, 19 (2015) 661-666.
63. R. Bashyam, M. Thekkumalai, V. Sivanandham, Evaluation of Phytoconstituents of Bryonopsis laciniosa fruit by UV-Visible Spectroscopy and FTIR analysis, Pharmacognosy Journal, 7 (2015).
64. U. Khandekar, A. Bobade, R. Ghongade, Evaluation of antioxident activity, in-vitro antimicrobial activity and phytoconstituents of Schleichera oleosa (Lour.) Oken, Int J Biol Pharm Res, 6 (2015) 137-143.
65. P. Azmath, S. Baker, D. Rakshith, S. Satish, Mycosynthesis of silver nanoparticles bearing antibacterial activity, Saudi Pharmaceutical Journal, 24 (2016) 140-146.
66. A.U. Khan, Q. Yuan, Y. Wei, K. Tahir, S.U. Khan, A. Ahmad, S. Khan, S. Nazir, F.U. Khan, Ultra-efficient photocatalytic deprivation of methylene blue and biological activities of biogenic silver nanoparticles, Journal of Photochemistry and Photobiology B: Biology, 159 (2016) 49-58.
67. E.O. Mikhailova, Silver nanoparticles: Mechanism of action and probable bio-

application, Journal of functional biomaterials, 11 (2020) 84.
68. I. Shahzadi, S.M. Aziz Shah, M.M. Shah, T. Ismail, N. Fatima, M. Siddique, U. Waheed, A. Baig, A. Ayaz, Antioxidant, cytotoxic, and antimicrobial potential of silver nanoparticles synthesized using Tradescantia pallida extract, Frontiers in Bioengineering and Biotechnology, 10 (2022) 907551.
69. Y. Gong, F. Fang, X. Zhang, B. Liu, H. Luo, Z. Li, X. Zhang, Z. Zhang, X. Pang, B type and complex A/B type epicatechin trimers isolated from litchi pericarp aqueous extract show high antioxidant and anticancer activity, International Journal of Molecular Sciences, 19 (2018) 301.
70. M. Narayanan, S. Divya, D. Natarajan, S. Senthil-Nathan, S. Kandasamy, A. Chinnathambi, T.A. Alahmadi, A. Pugazhendhi, Green synthesis of silver nanoparticles from aqueous extract of Ctenolepis garcini L. and assess their possible biological applications, Process Biochemistry, 107 (2021) 91-99.
71. S. Devanesan, M.S. AlSalhi, Green synthesis of silver nanoparticles using the flower extract of Abelmoschus esculentus for cytotoxicity and antimicrobial studies, International journal of Nanomedicine, 16 (2021) 3343.
72. J. Bhandari, B. Muhammad, P. Thapa, B.G. Shrestha, Study of phytochemical, anti-microbial, anti-oxidant, and anti-cancer properties of Allium wallichii, BMC Complementary and Alternative medicine, 17 (2017) 102.
73. E. Padilla-Camberos, K.J. Juárez-Navarro, I.M. Sanchez-Hernandez, O.R. Torres-Gonzalez, J.M. Flores-Fernandez, Toxicological Evaluation of Silver Nanoparticles Synthesized with Peel Extract of Stenocereus queretaroensis, Materials, 15 (2022) 5700.